Synthesis, Conformational Properties, and Immunogenicity of a Cyclic Template-Bound Peptide Mimetic Containing an NPNA Motif from the Circumsporozoite Protein of *Plasmodium falciparum*

Christian Bisang,[‡] Luyong Jiang,[‡] Ernst Freund,[‡] Fabienne Emery,[‡] Christian Bauch,[§] Hugues Matile,[§] Gerd Pluschke,[§] and John A. Robinson*,[‡]

Contribution from the Institute of Organic Chemistry, University of Zürich, Winterthurerstrasse 190, 8057 Zürich, and Swiss Tropical Institute, Socinstrasse 57, 4002 Basel, Switzerland

Received February 9, 1998

Abstract: The immunodominant central portion of the circumsporozoite (CS) surface protein of the malaria parasite *Plasmodium falciparum* contains a tetrapeptide motif, Asn-Pro-Asn-Ala (NPNA), tandemly repeated almost 40 times. The three-dimensional structure of the CS protein, including the central repeat region, is presently unknown. We have investigated an approach to stabilize β-turns in a single NPNA motif, by its incorporation into a template-bound cyclic peptide comprising the sequence ANPNAA. The template was designed to stabilize β-turns in the peptide loop and to allow its conjugation to T-cell epitopes in a multiple-antigen-peptide. NMR studies and MD simulations with time-averaged NOE-derived upper distance restraints support the formation of a stable β-I turn conformation in the NPNA motif of this template-bound antigen. Balb/c mice immunized with a multiple-antigen-peptide containing four copies of the template-bound loop conjugated to a single universal T-cell epitope produced antibodies that bound *P. falciparum* sporozoites in immunofluorescence assays. These results provide further support for the immunological relevance of a type-I β-turn conformation based on the NPNA cadence in the repeat region of the CS protein and illustrate the use of a novel template for the evaluation of conformationally constrained peptide immunogens.

Introduction

Plasmodium falciparum is the most virulent of the Plasmodial parasites that cause malaria. Infection of human hosts is initiated by the sporozoite stage, which is injected into the circulation following attack by infested mosquitoes. The sporozoites migrate to the liver where a specific ligand−receptor interaction, mediated by one of the major surface membrane proteins on the parasite, the circumsporozoite (CS) protein, may lead to invasion of liver cells.[1] One approach to develop a malaria vaccine is based on the observation that antibodies against the CS protein are able to block infection by sporozoites.[2,3] Although several B-cell epitopes have been described on the ca. 45 kDa CS protein,[4] the immunodominant response is directed against a central repeat region (approximately residues 150−300) comprising a motif Asn-Pro-Asn-Ala (NPNA), which is tandemly repeated almost 40 times. The role of the CS protein in protective immunity has been demonstrated in rodent models, using synthetic peptides,[5] recombinant proteins,[6] and immunization with DNA.[7] Nevertheless, the protective effect in humans of vaccination with peptides and proteins containing NPNA repeats was initially disappointing.[3] Recently, however, with the use of a more potent adjuvant, almost complete resistance to malaria infection was achieved in a Phase I trial using a recombinant protein vaccine comprising residues 207−395 of the CS protein.[8]

An important question concerns the conformation of the NPNA-repeat region in the intact CS protein. Earlier NMR studies of linear peptides containing tandemly repeated NANP and NPNA tetrapeptide motifs indicated the presence of conformers containing helical and/or reverse turns based on the NPNA cadence, in rapid dynamic equilibrium with unfolded forms.[9] Based on sequence preferences for β-turns in protein crystal structures,[10] a type-I β-turn seems a likely conformation for the NPNA motif in aqueous solution. A significant stabilization of β-I conformations was achieved by substituting proline by (*S*)-α-methylproline (P^{Me}) in linear peptides containing single and tandemly repeated ($NP^{Me}NA$) motifs.[11] Moreover, anti-$(NP^{Me}NA)_3$ antibodies raised in rabbits were able to bind to *P. falciparum* sporozoites in a solid-phase immuno-

* Corresponding author. Tel: (++)-41-1-635-4242. Fax: (++)-41-1-635-6812. E-mail: robinson@oci.unizh.ch.

‡ University of Zurich.

§ Swiss Tropical Institute.

(1) Cerami, C.; Frevert, U.; Sinnis, P.; Takacs, B.; Clavijo, P.; Santos, M. J.; Nussenzweig, V. *Cell* **1992**, *70*, 1021.

(2) Nardin, E. H.; Nussenzweig, R. S. *Annu. Rev. Immunol.* **1993**, *11*, 687.

(3) Nussenzweig, V.; Nussenzweig, R. S. *Adv. Immunol.* **1989**, *45*, 283.

(4) Calvo-Calle, J. M.; Nardin, E. H.; Clavijo, P.; Boudin, C.; Stuber, D.; Takacs, B.; Nussenzweig, R. S.; Cochrane, A. H. *J. Immunol.* **1992**, *149*, 2695−2701.

(5) Nardin, E. H.; Oliveira, G. A.; Calvo-Calle, J. M.; Nussenzweig, R. S. *Adv. Immunol.* **1995**, *60*, 105−149.

(6) Romero, P. *Curr. Opin. Immunol.* **1992**, *4*, 432−441.

(7) Sedegah, M.; Hedstrom, R.; Hobart, P.; Hoffman, S. L. *Proc. Natl. Acad. Sci. U.S.A.* **1994**, *91*, 9866−9870.

(8) Stoute, J. A.; Slaoui, M.; Heppner, D. G.; Momin, P.; Kester, K. E.; Desmons, P.; Wellde, B. T.; Garcon, N.; Krzych, U.; Marchand, M.; Ballou, W. R.; Cohen, J. D. *New Engl. J. Med.* **1997**, *336*, 86−91.

(9) Dyson, H. J.; Satterthwait, A. C.; Lerner, R. A.; Wright, P. E. *Biochemistry* **1990**, *29*, 7828−7837.

(10) Hutchinson, E. G.; Thornton, J. M. *Protein Sci.* **1994**, *3*, 2207−2216.

(11) Bisang, C.; Weber, C.; Inglis, J.; Schiffer, C. A.; van Gunsteren, W. F.; Jelesarov, I.; Bosshard, H. R.; Robinson, J. A. *J. Am. Chem. Soc.* **1995**, *117*, 7904−7915.

S0002-7863(98)00444-2 CCC: $15.00
Published on Web 07/17/1998

fluorescence assay, thus providing evidence for the biological relevance of the β-I conformation in the context of the folded CS protein. More recently, molecular dynamics simulations employing time-averaged NOE distance and ^3J-coupling constant restraints confirmed these structural conclusions and suggested how a compact folded structure might arise in $(NP^{Me}NA)_3$ peptides, by stacking of the proline rings in the outer two motifs to form a hydrophobic core.[12] Similarly folded forms would also be possible in longer tandemly repeated NPNA peptides, thereby forming a stemlike structure, which conceivably might also occur in the native CS protein.

In earlier work, Satterthwait et al.[13] synthesized conformationally constrained variants of $(NPNA)_3$ in which the side chains of two Asn residues, flanking either Pro or Ala, were joined by ethylene bridges and showed that the former could elicit anti-sporozoite antibodies in rabbits. This was the first demonstration that nonproteinogenic conformational constraints could be used to prepare effective immunogens, although the conformations stabilized by these modifications were not described.

In this work, we have investigated an alternative approach to stabilize a β-I turn in the NPNA motif within a template-bound cyclic peptide comprising the sequence ANPNAA. The template was designed to stabilize β-turns in the peptide loop and to allow its presentation to the immune system as a conformationally constrained peptide immunogen conjugated to T-cell epitopes in a multiple-antigen-peptide format.[14] An optimized route to the template **1** and peptide antigen **2** is

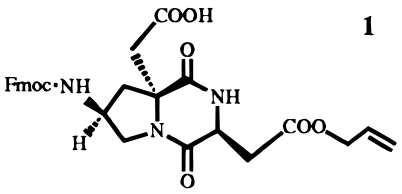

1

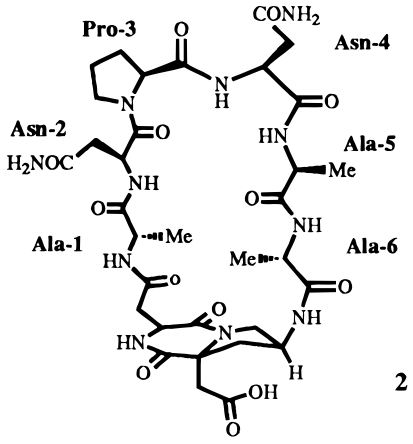

2

presented,[15] that allows the convenient preparation of **1** on a gram scale. In addition, conformational studies on **2** are described, based on NMR and MD simulations with time-averaged distance restraints. Finally, we report that the multiple-antigen-peptide **9**, incorporating **2**, is able to elicit antibodies in mice that cross-react with *P. falciparum* sporozoites, under conditions where a linear peptide containing the same epitope fails to elicit a detectable anti-sporozoite antibody response.

Scheme 1[a]

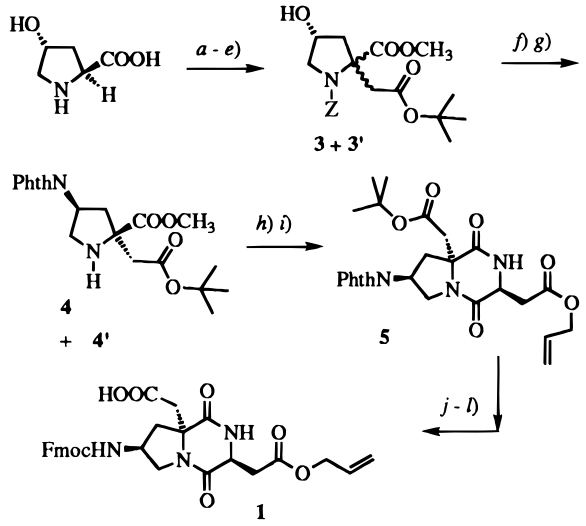

[a] Reagents: *a*) $SOCl_2$, MeOH, 93%; *b*) BnOCOCl, Na_2CO_3 aqueous 1 M/dioxane, 84%; *c*) TMSCl, NEt_3, THF; *d*) LDA, $BrCH_2CO_2{}^tBu$, THF; *e*) citric acid 10%, MeOH, 72% over three steps; *f*) Ph_3P, PhthNH, DEAD, THF, 74%; *g*) Pd/C, H_2, 47%; *h*) Fmoc-Asp(OAllyl)-OH, DCC, HOAt, CH_2Cl_2; *i*) DBU 5%, MeCN, 64% over two steps; *j*) $MeNHNH_2$, DMF; *k*) Fmoc-Succ, imidazole, DMAP, DCM, 58% over two steps; *l*) DCM, TFA 1:2, 97%.

Results

Design and Synthesis. The template **1** can be readily synthesized on a gram scale using the route shown in Scheme 1, which has been optimized from that described previously in a communication.[15] The alkylation of Me_3Si-protected *N*-Z-4-hydroxyproline methyl ester can be performed conveniently on a large scale and after removal of the temporary Si-protecting group gives the desired diastereomer in about 2:1 (**3**:**3′**) excess. After a Mitsunobu reaction[16] and removal of the Z protecting group, the desired stereoisomer **4** could be obtained easily by a simple recrystallization, without the need for large scale chromatography. The relative configuration of **4** was confirmed by steady-state NOE-difference experiments. The coupling of **4** with Fmoc-Asp(allyl)-OH proceeded in good yield using DCC and HOAt for activation. The resulting dipeptide could then be cyclized directly to give **5**, and exchange of protecting groups yielded the template **1** in a form suitable for solid-phase peptide synthesis.

To assemble the cyclic antigen **2** on a solid-phase (Scheme 2), the template **1** was coupled to Tentagel S-AC resin through the free carboxylic acid, and the linear peptide chain was then assembled using standard Fmoc-chemistry.[17] The allyl ester of the template was cleaved using Pd^0, and cyclization was accomplished with BOP and DIEA in NMP-DMSO. The products of the cyclization were analyzed by reverse-phase HPLC following cleavage from the resin and deprotection with TFA. Two major products were detected in approximately 2:1 ratio. Electrospray mass spectrometry indicated they were the desired product (30% yield) (MS: 806.5 $[(M + H)^+]$), and a dimeric species (MS: 1612 $[(M + H)^+]$) that was not investigated further. Alternatively, cleavage from the resin with

(12) Nanzer, D.; Torda, A. E.; Bisang, C.; Weber, C.; Robinson, J. A.; van Gunsteren, W. F. *J. Mol. Biol.* **1997**, *267*, 1011−1024.

(13) Satterthwait, A. C.; Arrhenius, T.; A., H. R.; Zavala, F.; Nussenzweig, V.; Lerner, R. A. *Philos. Trans. R. Soc. B* **1989**, *323*, 565−572.

(14) Tam, J. P. *J. Immunol. Methods* **1996**, *196*, 17−32.

(15) Emery, F.; Bisang, C.; Favre, M.; Jiang, L.; Robinson, J. A. *J. Chem. Soc., Chem. Commun.* **1996**, 2155−2156.

(16) Mitsunobu, O.; Wada, M.; Sano, T. *J. Am. Chem. Soc.* **1972**, *94*, 679−680.

(17) Atherton, E.; Sheppard, R. C. *Solid-phase peptide synthesis − a practical approach*; IRL Press: Oxford, 1989.

1% TFA in CH_2Cl_2 gave **7** with the side chain protecting groups intact. The peptide **8** was synthesized in a similar way, and the disulfide bridge was introduced in the last step by aerial oxidation of the corresponding dithiol.

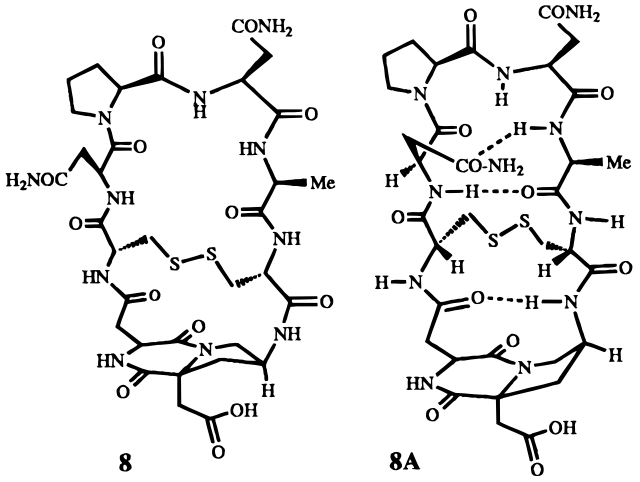

8 **8A**

For immunizations, the multiple antigen peptides **9** and **10** were prepared by straightforward solid-phase methods using Fmoc-chemistry. The final steps in the assembly of **9** involved coupling **2** to resin bound H_4-Lys$_2$-Lys-Ala.Ala.Gln(Mtt).Tyr(*t*Bu).Ile.Lys(Boc).Ala.Asn(Mtt).Ser(*t*Bu).Lys(Boc).Phe.Ile.Gly.Ile.Thr(*t*Bu).Glu(O*t*Bu).Leu.Ala-O−Resin, which was performed with a 4-fold excess of **2** and HBTU/HOBt for activation. Both **9** and **10** were purified by HPLC and gave electrospray mass spectra consistent with their predicted masses.

NMR and Conformational Studies. The aim of these studies was to determine which conformations are preferred in the cyclic peptide antigen **2**. The peptide **8** served here as a useful reference. All studies were performed in aqueous solution. The chemical shifts and ^{1}H NMR line widths of **2** and **8** remain unchanged in H_2O/D_2O (90:10, pH 5) in the concentration range 10.0−0.3 mM, indicating an absence of aggregation. The chemical shift assignments were made by standard methods[18] and are given in Table 1 and 2.

Chemical Shifts and Chemical Exchange. The amide region of the ^{1}H NMR spectrum of **2** revealed the presence of a minor conformer, representing ca. 10% of the major conformer. Chemical exchange between the major and minor forms

Scheme 2[a]

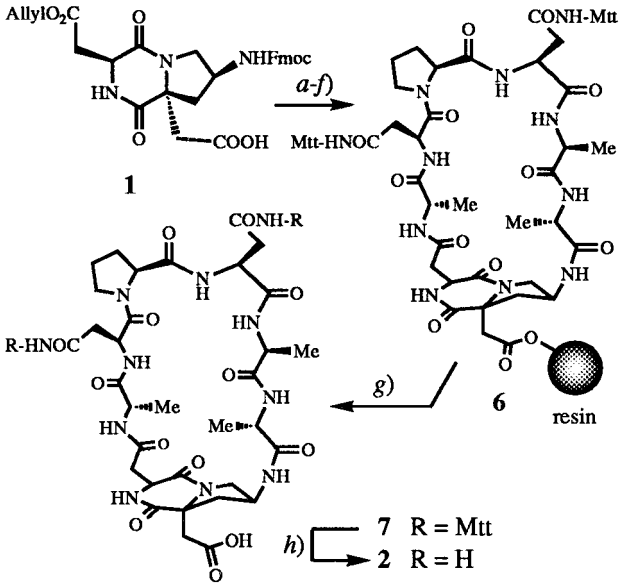

[a] Reagents: *a*) **1** (2 equiv), Tentagel-SAC, CIP (6 equiv), Pyr/CH_2Cl_2; *b*) piperidine, DMF; *c*) peptide assembly using HBTU (3 equiv), HOBt (3 equiv) in DMF, DIEA, and Fmoc-protected amino acid (3 equiv) in each coupling step, piperidine in DMF for Fmoc-removal; then *d*) $Pd(PPh_3)_4$ (3 equiv), NMM, AcOH, DMF; *e*) piperidine, DMF; *f*) BOP (1.5 equiv), DIEA (3.0 equiv), NMP, DMSO; *g*) 1% TFA/CH_2Cl_2 (≈30% yield over last four steps); *h*) 95% TFA.

could be seen in ROESY spectra at 300 K as cross-peaks with the same positive sign as the diagonal. The rates of interconversion of these conformers were calculated from the ratio of the intensity of the diagonal (I_{AA}) and exchange cross-peaks (I_{AB}) for the NH signals, which are related to the rate of exchange (k) according to eq 1[19]

$$I_{AA}/I_{AB} = [(1/k) \times (1/t_m)] - 1 \qquad (1)$$

where t_m is the mixing time. From the gradient of a plot of I_{AA}/I_{AB} versus $1/t_m$ (ROESY mixing times were 75, 150, 225, and 300 ms) the exchange rates were estimated to be $k_{(major->minor)} = 0.011\ s^{-1}$ and $k_{(minor->major)} = 0.12\ s^{-1}$. The exchange cross-peaks are not apparent in ROESY spectra measured at 285 K, indicating that the exchange rate is slower than the mixing period at this temperature. Earlier ^{1}H NMR spectra of linear peptides

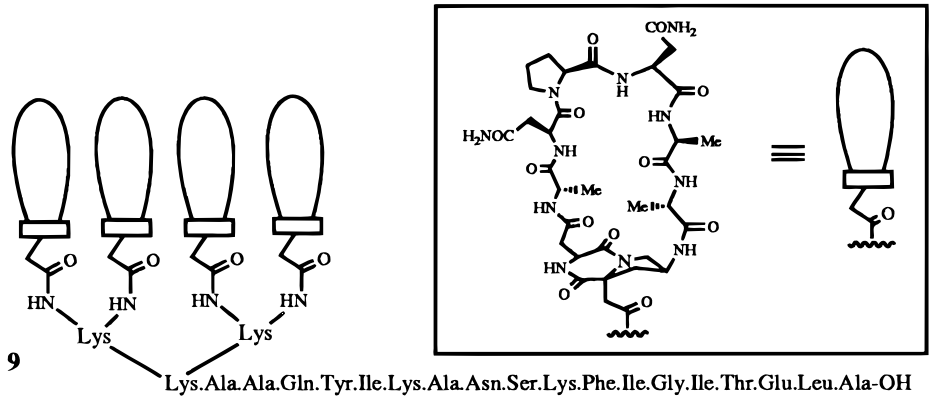

9 Lys.Ala.Ala.Gln.Tyr.Ile.Lys.Ala.Asn.Ser.Lys.Phe.Ile.Gly.Ile.Thr.Glu.Leu.Ala-OH

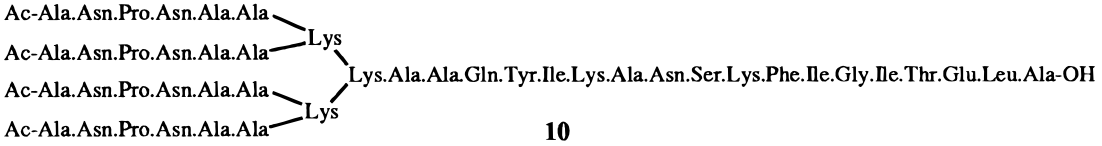

10

Table 1. ^{1}H NMR (600 MHz) Chemical Shifts for **2** at 300 K in 10% $^2H_2O/H_2O$, pH = 5.0

		chemical shift[a] (ppm)		
residue	NH	H−C$_\alpha$	H−C$_\beta$[b]	others
Ala^1	8.34 8.07[c]	4.29	1.31	
Asn^2	8.13 7.69[c]	4.93	2.64, 3.15	NH(δ)^E 7.46, NH(δ)^Z 7.06
Pro^3		4.42	1.96, 2.32	CH$_2$(γ) 1.97, 2.02; CH$_2$(δ) 3.78
Asn^4	8.41 8.53[c]	water[d]	2.72, 2.88	NH(δ)^E 7.65, NH(δ)^Z 6.98
Ala^5	7.60 8.52[c]	4.38	1.28	
Ala^6	8.21 7.97[c]	4.30	1.33	
Pro(NH$_2$)^7 [e]	8.46 7.74[c]		*1.96, 2.60*[b]	CH$_2$(δ) 3.82, 3.87 CH$_2$(ϵ) 2.75, 2.66
Asp^8	8.30 8.11[c]	4.45	*2.80, 3.26*[b]	

[a] Chemical shifts are measured relative to internal TSP [sodium(trimethylsilyl)-d_4-propionate]. Pro(NH$_2$)^7 and Asp^8 are the 4-aminoproline and aspartate moieties of the template. [b] Stereospecific assignments are in *italics*, in the order pro-*R*, pro-*S*. [c] The peptide NH assignments for the minor conformer (see text). [d] Resonance lies under the water signal. [e] The Pro(NH$_2$)^7 NH refers to NH-C(γ). The Pro(NH$_2$)^7 H-C(γ) lies under the water signal.

Table 2. ^{1}H NMR (600 MHz) Chemical Shifts for **8** at 300 K in 10% $^2H_2O/H_2O$, pH = 5.0

		chemical shift[a] (ppm)		
residue	NH	H−C$_\alpha$	H−C$_\beta$[b]	others
Cys^1	8.78	5.32	3.01, 2.94	
Asn^2	8.65	5.00	3.18, 2.88	NH(δ)^E 7.70, NH(δ)^Z 6.95
Pro^3		4.26	2.42, 1.75	CH$_2$(γ) 2.13, 1.96; CH$_2$(δ) 3.86, 3.67
Asn^4	8.52	4.75[c]	2.86, 2.79	NH(δ)^E 7.58, NH(δ)^Z 6.95
Ala^5	7.86	4.48	1.36	
Cys^6	8.67	5.20	3.07, 2.89	
Pro(NH$_2$)^7 [d]	8.84		*2.35, 2.54*[b]	CH$_2$(δ) *3.49, 4.14*;[b] CH(γ) 4.52; CH$_2$(ϵ) 2.83, 2.71
Asp^8	8.29	4.53	*2.97, 3.35*[b]	

[a] Chemical shifts are measured relative to internal TSP [sodium(trimethylsilyl)-d_4-propionate]. Pro(NH$_2$)^7 and Asp^8 are the 4-aminoproline and aspartate moieties of the template. [b] Stereospecific assignments are in *italics*, in the order pro-*R*, pro-*S*. [c] Resonance lies under the water signal. [d] The Pro(NH$_2$)^7 NH refers to NH−C(γ).

containing tandemly repeated NPNA motifs also revealed major and minor conformers in about the same ratio,[9] due to *cis*−*trans* isomerism at one or more Asn-Pro peptide bonds, whereas (NP^{Me}NA)$_3$ peptides showed a single average structure by NMR.[11] The ^{1}H NMR spectrum of **8** also revealed only a single species on the NMR chemical shift time scale at 300 K.

Since correlations between chemical shift and peptide secondary structure are currently of general interest, we note here that the Ala^5 NH in **2** and **8** resonates considerably upfield from the random coil value at this temperature,[20] the former by +0.88 ppm and the latter by +0.62 ppm. Moreover, in **8**, the H−C(α) resonances of Cys^1, Cys^6, and Asn^2 are appreciably downfield shifted compared to the random coil values, in the case of Cys^1 by −0.74 ppm.

The temperature coefficients of the amide NH resonances for **2** and **8** are collected in Table 3. The low value for Ala^5 NH suggests significant shielding from solvent. The relative exchange rates of amide NH protons were measured by monitoring the disappearance of resonances upon dissolution in D_2O at 293 K. For **2**, the peptide NH protons for Asn^4 and Ala^5 NHs exhibited half-lives of ca. 12 and 25 min, respectively, at pH 3.4, whereas the others exchanged completely within a few minutes. A similar pattern was noted earlier in a closely related system.[21] For **8**, a different result was observed, with Pro(NH$_2$)^7 NH−C(γ) now exchanging very slowly ($t^1/_2$ = >24 h) at pH 4.0, followed by Asn^2 NH ($t^1/_2$ = 90 min) and Ala^5 NH ($t^1/_2$ = 66 min). The other NH protons again exchanged completely within a few minutes, and their exchange rates presumably approximate to random coil values under these conditions.

Coupling Constants. The ^3J (α,β) coupling constants for the Asn^2 and Asn^4 residues in **2** (Table 4) have combinations of high and low values, indicative of preferred conformations for each side chain. Rotational averaging, if dominant, would result in both values being close to 6.5 Hz, which is not observed. In **8**, however, a different preferred conformation is populated by the Asn^2 side chain, since both ^3J (α,β) values are now small. Peptide **8** is expected to be more rigid than **2**, and the other coupling constants support this. For example, several ^3J (α,NH) values are > 9.0 Hz, and all other ^3J coupling constants have nonaveraged values. This includes ^3J (α,β), ^3J (β,γ), and ^3J (γ,δ) for the aminoproline and aspartate moieties of the template. In contrast, the aminoproline moiety of the template in **2** shows ^3J (β,γ) and ^3J (γ,δ) values in the range 5−8 Hz, which for a proline residue indicate rapid fluctuations in ring pucker.[22] In both **2** and **8**, the combination of two small ^3J (α,β) values for the aspartate moiety of the template indicate a preferred torsion angle χ_1 around +60°.

NOEs and Structure Calculations. A summary of the NOEs observed in **2** are shown in Figure 1. Noteworthy are the medium range (i, i+2) and (i, i+3) NOE connectivities within the four residues of the NPNA motif as well as a relatively strong Asn^4-Ala^5 d_{NN} NOE, which together are characteristic of a highly populated β-turn conformation with proline at the (i+1) position. The low-temperature coefficient of the Ala^5 NH proton (Table 3) and its relatively slow H/D exchange rate (see above) are also consistent with a β-turn in the NPNA motif stabilized by H-bonding involving the Ala^5 amide proton. Although a β-I turn appears to be favored (vide infra), the observation of a medium strength Pro^3-Asn^4 $d_{\alpha N}$ (i, i+1) NOE indicates a shorter Pro^3 H−C(α) to Asn^4 NH distance than seen in an ideal β-I turn, most likely due to torsional motion involving this amide plane or occasional flipping to a type-II β-turn.

Average solution structures were calculated for **2** based on upper-distance and one dihedral angle restraint (Asp^8 χ_1 = 60 ± 30°) using a simulated annealing (SA) method.[21] From 30 calculations, 27 structures were within 10 kcal/mol of the minimum energy structure and showed no distance restraint violations > 0.3 Å; for nine of these structures, the violations were < 0.25 Å. The final 27 SA structures revealed structural convergence to a family of closely related backbone conformations with a pairwise rms deviation for superimposition of the backbone N, C(α), and C′ atoms in all residues of 0.43 ± 0.32 Å. The minimum energy structure is shown in Figure 2A. Only one distance restraint, that derived from the Pro^3-Asn^4 $d_{\alpha N}$ (i, i+1) NOE, was consistently violated in the range 0.2−0.3 Å.

(18) Wüthrich, K. *NMR of proteins and nucleic acids*; Wiley-Interscience: New York, 1986.
(19) Ernst, R. R.; Bodenhausen, G.; Wokaun, A. *Principles of NMR spectroscopy in one and two dimensions*; Clarendon Press: Oxford, 1987.
(20) Merutka, G.; Dyson, H. J.; Wright, P. E. *J. Biomol. NMR* **1995**, *5*, 14−24.
(21) Bisang, C.; Weber, C.; Robinson, J. A. *Helv. Chim. Acta* **1996**, *79*, 1825−1842.
(22) Mádi, Z. L.; Griesinger, C.; Ernst, R. R. *J. Am. Chem. Soc.* **1990**, *112*, 2908−2914.

Table 3. Amide Temperature Coefficients for **2** and **8**

Temperature Coefficients[a] for Peptide **2**											
Residue	Ala[1]	Asn[2]	NH^E	NH^Z	Asn[4]	NH^E	NH^Z	Ala[5]	Ala[6]	Pro(NH$_2$)[7]	Asp[8]
$-\Delta\delta$/K [ppb/K]	7.6	6.8	3.8	6.3	4.5	6.5	6.3	1.2	6.5	7.4	8.4
Temperature Coefficients[a] for Peptide **8**											
Residue	Cys[1]	Asn[2]	NH^E	NH^Z	Asn[4]	NH^E	NH^Z	Ala[5]	Cys[6]	Pro(NH$_2$)[7]	Asp[8]
$-\Delta\delta$/K [ppb/K]	7.9	2.1	5.3	4.4	4.6	6.4	5.5	2.8	7.4	3.0	9.0

[a] The coefficients for the peptide amides and the side chain NHs of Asn are given. Measurements were made in aqueous solution (10% D_2O/H_2O, pH 5) in the range 5−41°.

Table 4. Coupling Constants[a] (Hz) for **2** and **8**

residue	^3J (α,NH)	^3J (α,β)	others
		2	
Ala[1]	5.8	7.0	
Asn[2]	7.3	4.3, 9.9[b]	J (β,β′) 15.0
Pro[3]		4.7, 8.8[b]	n.d.
Asn[4]	8.8	10.5, 4.5[b]	J (β,β′) 15.1
Ala[5]	6.7	7.0	
Ala[6]	6.2	7.1	
Pro(NH$_2$)[7]	8.5[c]		J (β_R,γ) 8.0, J (β_S,γ) 7.5, J (β,β′) 12.5, J (γ,δ) 5.7,[b] J (γ,δ′) 8.9,[b] J (δ,δ′) 13.2, J (ε,ε′) 15.1
Asp[8]	<3.0	4.7, 2.7[d]	J (β,β′) 16.9
		8	
Cys[1]	9.5	4.3, 10.4	J (β,β′) 15.2
Asn[2]	8.7	3.9, 5.4[b]	J (β,β′) 15.8
Pro[3]		7.0, 10.8[b]	n.d.
Asn[4]	9.1	10.1, 5.4[b]	J (β,β′) 14.7
Ala[5]	6.2	6.8	
Cys[6]	9.8	4.6, 10.6	J (β,β′) 15.1
Pro(NH$_2$)[7]	9.8[c]		J (β_R,γ) < 2.0, J (β_S,γ) 7.3, J (β,β′) 15.0, J (γ,δ_R) 4.2, J (γ,δ_S) < 2.0, J (δ,δ′) 12.8, J (ε,ε′) 15.6
Asp[8]	<2.0	3.9, 3.1[d]	J (β,β′) 18.0

[a] Measured from 1D and/or E.COSY spectra. [b] Stereospecific assignments not available. [c] Refers to the ^3J(NH−C(γ), H−C(γ)) coupling. [d] Given in the order pro-*R*, pro-*S*.

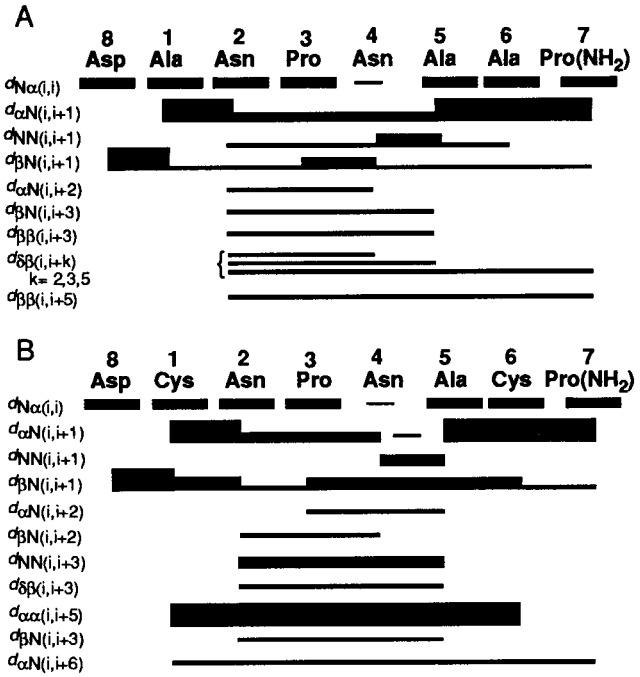

Figure 1. Summary of key NOE connectivities found for (A) peptide **2** and (B) peptide **8**. The Asn[4] H−C(α) lies under the water signal. NOE connectivities with Pro[3] are to the H−C(δ)'s in place of NH. Pro(NH$_2$)[7] NH refers to the NH−C(γ) in the aminoproline moiety of the template.

However, all the SA structures have the NPNA motif in a type-I β-turn, whereas as noted above, torsional motion of the amide plane or flipping to a type-II turn would lead to a shorter Pro[3] H−C(α) to Asn[4] NH distance. In addition, all the SA structures have the same ring pucker for the aminoproline moiety of the template, with $\chi_1 \approx -35°$, yet the ^3J coupling constants within this ring provide evidence for flipping of ring pucker.

The pattern of NOE connectivities observed in peptide **8** (see Figure 1), in particular the strong Cys[1]-Cys[6] $d_{\alpha\alpha}$ (i, i+5) and Asn[2]-Ala[5] d_{NN} (i, i+3) NOEs, provides evidence for a β-hairpin conformation from Cys[1]-Cys[6], and this is borne out by structure calculations. Of 30 structures generated by SA using NOE-derived distance restraints, 25 were within 10 kcal/mol of the global minimum and showed no NOE violations >0.2 Å. Moreover, these structures converged to a family of closely related conformers having a β-hairpin backbone conformation (with a pairwise rms deviation for superimposition of the backbone N, C(α), and C′ atoms in all residues of 0.38 ± 0.20 Å) as seen in the energy minimized SA structure deduced for **8** shown in Figure 2B. The final 25 SA structures all possess a type-I β-turn in the NPNA motif, and the side chain Asn[2] O(δ) is frequently found H-bonded to the Ala[5] backbone NH, as was observed also for **2** (Figure 2A). The residues Cys[1]-Pro[3] and Asn[4]-Cys[6] form two β-strands, connected at Pro[3]-Asn[4] by the β-turn, with the hairpin stabilized by the template, and the Cys[1]-Cys[6] disulfide bridge. Hydrogen bonds may form between the backbone amides in opposing β-strands as indicated by the dotted lines in **8A** (see also Figure 2B) which is consistent with both the low-temperature coefficients (Table 2) and slow H/D exchange behavior (vide supra) of these (Asn[2], Ala[5], and Pro(NH$_2$)[7]) NH protons. ^3J (α,NH) values ≈ 9.0 Hz are also consistent with a β-hairpin conformation. The nonaveraged ^3J (α,β) values indicate a relatively well defined conformation for each of the Asn and Cys side chains and are consistent with those found in the SA-structures (Figure 2B). The ^3J (β,γ) and ^3J (γ,δ) values for the aminoproline moiety of the template are also consistent with the observed χ_1 values of ≈+10−12°, which places the N−C(γ) substituent in a pseudoaxial position. Taken together, the NMR data suggest that to a reasonable approximation the peptide **8** may be viewed as a relatively rigid molecule, undergoing mostly small amplitude motion about backbone and side chain dihedral angles.

Although the NMR data indicate stable secondary structure in the backbone of **2**, this molecule is not rigid but rather retains a significant degree of flexibility which may include flipping of pyrrolidine rings and amide planes (vide supra). An attempt to account for flexibility in the structure calculations for **2** was made by incorporating the atom−atom upper distance restraints as values that are to be fulfilled, not instantaneously, but over the course of an MD simulation with solvent water present, i.e., as time-averaged distance restraints (TA-DR).

The energy minimum SA structure found for **2**, embedded in a bath of water molecules, was taken as a starting point for 2 ns MD simulations at 300 K, performed with the 43A1 force

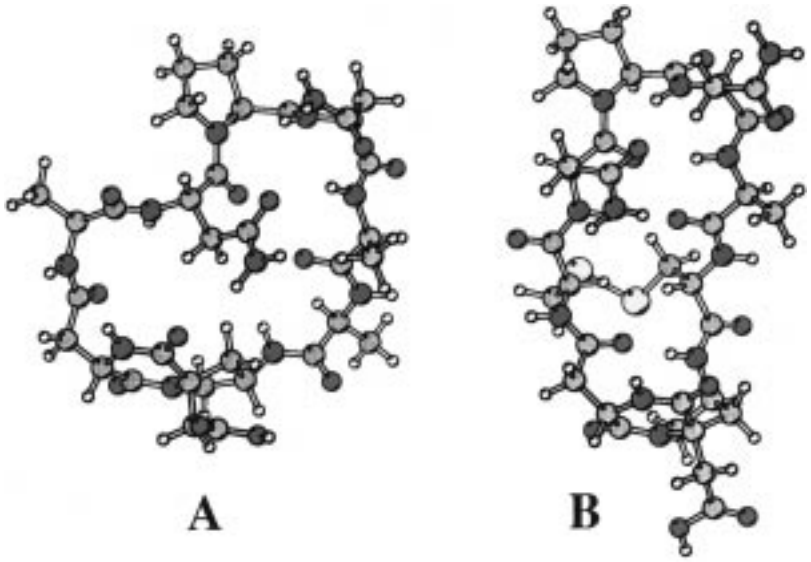

Figure 2. (A) Energy minimum structure deduced by dynamic simulated annealing for peptide **2**. (B) Energy minimum structure deduced by dynamic simulated annealing for peptide **8**. Yellow = S atoms, red = O atoms, blue = N atoms, gray = C atoms. The structures were drawn using Molscript.[37]

field in GROMOS96,[23] both with and without TA-DR. The results for both runs were similar (Table 5), indicating that the restraints are well satisfied by structures at and near to the energy minimum in this force field. A simulation with TA-DR was also performed with **2** as a Na^+-carboxylate salt, but again the results were not significantly different. Three parameters illustrate well the types of motion undergone by **2** during the simulation: (1) the Asn^2 C(α) to Ala^5 C(α) distance, which in a β-turn is less than 7 Å;[24] (2) the χ_1 value of the aminoproline moiety of the template, which is $\approx -35°$ in the starting SA structure (Figure 2A) but flips to $\approx +10-12°$ in the β-hairpin conformation seen in **8** (Figure 2B); and (3) the Pro^3 and Asn^4 ϕ/ψ angles, since these change from $\approx -60°/-30°$ and $-90°/0$ °C, respectively, in a β-I turn to $\approx -60°/+120°$ and $+80°/0$ °C in a β-II turn.[10,24]

The Asn^2 C(α) to Ala^5 C(α) distance in **2** remains ≈6 Å during almost the entire simulation, both with (Figure 3) and without TA-DR (data not shown). Moreover, the Pro^3 ϕ/ψ and Asn^4 ϕ angles remain for most of the simulation within ±30° of the values expected for a β-I turn (Figure 4); only very infrequently are conformers populated close to a β-II turn. The Pro^3 H−C(α) to Asn^4 NH upper distance restraint shows the largest single violation (Table 5). The variation of χ_1 in the aminoproline moiety of the template is shown in Figure 5. For most of the simulation the ring pucker remains in the range $\chi_1 \approx -30°$ to $-20°$, close to that in the starting structure ($\chi_1 \approx -35°$), with the N−C(γ) in a pseudoequatorial position. However, ring flips to a $\chi_1 > 0°$ are observed, which brings the N−C(γ) into a pseudoaxial position and the template and the peptide loop into a β-hairpin-like conformation (Figure 6), similar to that deduced for **8** (see Figure 2). A similar ring flipping was also seen in the unrestrained MD simulation of **2** (data not shown).

Immunological Studies. To investigate whether the cyclic mimetic **2** can elicit antibodies that bind to *P. falciparum* sporozoites, peptide **9** was prepared which contains also a promiscuous T-helper cell epitope.[25] As a control, the same ANPNAA epitope as a linear peptide was incorporated into the immunogen **10**. Groups of BALB/c mice were immunized five

Table 5. Results of the MD Simulation with TA-DR for Peptide **2**[a]

Part A

energies (kJ/mol)/temp (K)	av over the run	rms fluctuations
potential energy	−47 817	165
bond angle energy	137	17
improper dihedral energy	34	7.9
dihedral energy	81	11.7
electrostatic energy		
peptide−peptide	−430	27
peptide−solvent	−502	64
solvent−solvent	−54 990	323
LJ interaction energy		
peptide−peptide	−108	11
peptide−solvent	−202	21
solvent−solvent	8060	226
distance restraint energy	1.9	0.7
temperature	302.5	3.8

Part B

sum of violations of distance restraints (Å)	0.79
largest violation (Å)	0.53

Part C

hydrogen bonds (donor:acceptor)	%
Asn^2 HδE:Apro^7 O	23
Asn^2 HδZ:Apro^7 O	19
Asn^4 HN:Asn^2 Oδ	26
Ala^5 HN:Asn^2 Oδ	50
Apro^7 HN−C(γ):Asn^2 Oδ	11
Apro^7 HN−C(γ):Ala^5 O	3
Asn^2 HN:Asp^8 Oδ	2

[a] Part A, gives the average contributions to the total energy separated on the basis of terms in the force field and the rms fluctuations as well as the temperature. Part B gives the distance restraint violations. Part C shows the percentage population of hydrogen bonds to a cut-off of 2%. Apro^7 refers to the aminoproline moiety of the template. All values are taken over the entire 2 ns simulation.

(23) van Gunsteren, W. F.; Billeter, S. R.; Eising, A. A.; Hünenberger, P. H.; Krüger, P.; Mark, A. E.; Scott, W. R. P.; Tironi, I. G. *Biomolecular simulation: The GROMOS96 manual and user guide*; Hochschulverlag AG an der ETH Zurich: Zurich, 1996.

(24) Wilmot, C. M.; Thornton, J. M. *J. Mol. Biol.* **1988**, *203*, 221−232.

(25) Kumar, A.; Arora, R.; Kaur, P.; Chauhan, V. S.; Sharma, P. *J. Immunol.* **1992**, *148*, 1499−1505.

times subcutaneously with **9** or **10** together with the adjuvant QS-21. A control group received only the adjuvant. The development of IgG titers was monitored by ELISA (Figure 7). Mice immunized with **9** developed relatively low anti-**9** IgG titers, which increased slowly with each immunization. Serum antibodies of these mice did not react with **10** (Figure 7), indicating that **2** is the immunodominant determinant of **9**. No cross-reactivity with **9** developed in mice immunized with **10** or with adjuvant alone.

Cross-reactivity with *P. falciparum* sporozoites was tested with an immunofluorescence assay. None of the mice immunized with **10** or with adjuvant alone stained sporozoites. In contrast, staining was obtained with the serum of some of the 15 mice immunized with **9** (Figure 8). After three immunizations, one serum was positive, after four immunizations three sera were positive, and after an additional immunization 12 of 15 mice were positive. The specificity of the cross-reaction was analyzed by competition experiments. Incubation in the presence of the immunogen **9**, or the mimetic **2**, completely abolished the antibody reactivity of positive sera with sporozoites (Figure 8). Neither the immunogen **10** containing the linear epitope nor cyclic peptides with different sequences mounted on the template inhibited the binding of the cross-reactive anti-**9** antibodies to the sporozoites.

Discussion

The design of the template **1** represents an attempt to discover novel semirigid structural units that, in the context of a cyclic peptide, exert an influence on the peptide conformation and allow conjugation to other building blocks, including T-cell epitopes in a multiple-antigen-peptide suitable for immunizations.[14] The template itself is readily accessible and might prove to be generally useful in the evaluation of conformationally restrained B-cell epitopes.

The inherent flexibility of linear synthetic peptides is a well-known drawback in their use as synthetic vaccines, in particular for mimics of continuous conformational protein epitopes.[26] There is, however, increasing interest in the rational design of constrained synthetic peptide vaccines. Ideally, the backbone of the peptide should adopt conformations present in the epitope, on the intact protein, while bound to a neutralizing antibody. We chose to examine here a synthetic epitope comprising just four amino acids, NPNA, which occurs naturally in a tandemly repeated form in the CS protein of *P. falciparum*. The key issue in this case was to create a constrained and conformationally defined peptide that can elicit antibodies able to bind the parasite. Both linear and cyclic peptides containing multiple NPNA-motifs have been shown already to act in this way,[3,5,27,28] albeit with varying levels of effectiveness, but their preferred conformations are less well defined. An improved understanding of the secondary structure of the repeat region, and its sequence dependence, might be useful for the design of more effective synthetic malaria vaccines.

Since earlier studies had indicated that synthetic peptides containing tandemly repeated NANP and NPNA motifs populate β-I turns based on the NPNA cadence, in rapid dynamic equilibrium with unfolded forms,[9,11,12] we set out to stabilize this conformation in a single NPNA motif in the context of a cyclic peptide with template **1**. The cyclic peptide antigen **2**, with six amino acids attached to the template, was chosen for study, since modeling indicated that a β-I hairpin conformation

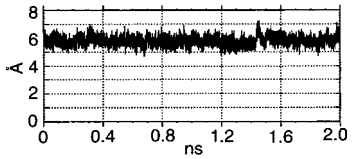

Figure 3. Interatomic distance Asn^2 C(α) to Ala^5 C(α) (Å) as a function of time during the MD simulation of **2** with TA-DR.

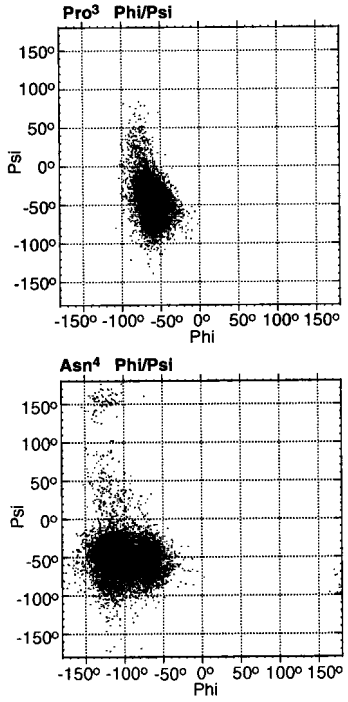

Figure 4. Ramachandran plot for the Pro^3 and Asn^4 residues taken every 0.2 ps during the 2 ns MD simulation of **2** with TA-DR.

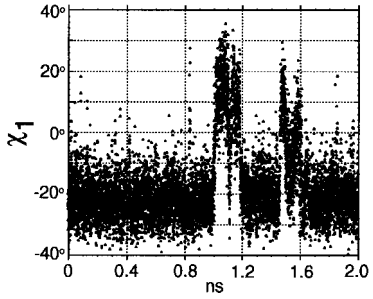

Figure 5. Plot of the χ_1 angle (N, C(α), C(β), C(γ) torsion) in the aminoproline moiety of the template as a function of time at 0.2 ps time steps during the MD simulation of **2** with TA-DR.

in the peptide backbone should be possible, whereas this would not be the case with only four residues attached to the template[21] (see Figure 2). Before any attempts to determine average solution structures were made, evidence for stable secondary structure was sought, based on analyses of chemical shifts, coupling constants, amide temperature coefficients, relative amide H/D exchange rates, and NOEs for both **2** and the more highly restrained peptide **8**. According to each of these parameters, a stable β-turn appeared to be significantly populated in both molecules (see Results section).

The predominance of a type-I β-turn in the NPNA motif in both **2** and **8** was indicated by SA structures calculated using NOE-derived upper distance restraints (Figure 2). The SA structure deduced for **8** is consistent with the NMR data, which supports our view of this molecule as being relatively rigid. However, some of the coupling constants observed for **2** are

(26) Brown, F. *Philos. Trans. R. Soc. London B* **1994**, *344*, 213-219.
(27) Etlinger, H. M.; Renia, L.; Matile, H.; Manneberg, M.; Mazier, D.; Trzeciak, A.; Gillessen, D. *Eur. J. Immunol.* **1991**, *21*, 1505−1511.
(28) Etlinger, H. M.; Trzeciak, A. *Philos. Trans. R. Soc. London B* **1993**, *340*, 69−72.

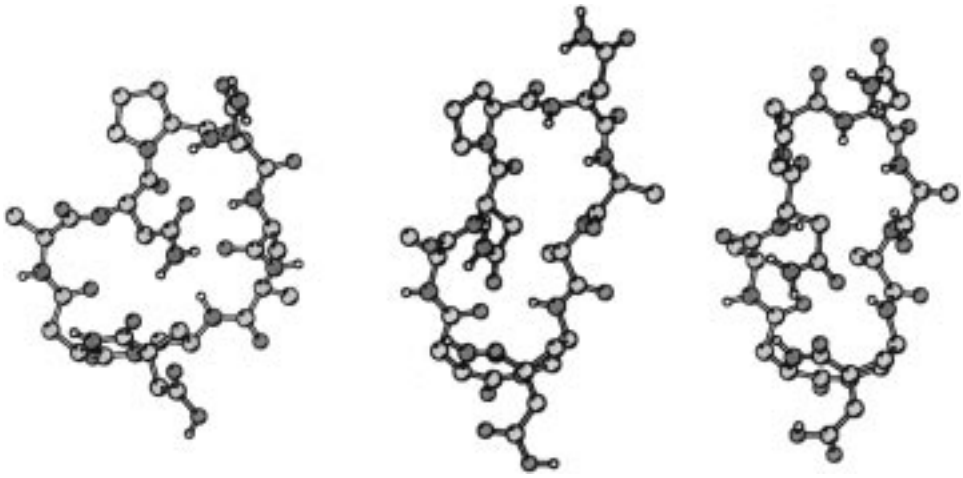

Figure 6. Snapshots taken from the MD simulation with TA-DR of **2** having different χ_1 angle in the aminoproline moiety of the template (Figure 5); *left*, at 1.7 ns ($\chi_1 = -37°$); *middle*, at 1.06 ns ($\chi_1 = +0.5°$); *right* at 1.04 ns ($\chi_1 = +20.5°$). H atoms except amide NHs are omitted for clarity. The structures were drawn using Molscript.[37]

inconsistent with the average structure determined by SA (Figure 2A). In an attempt to explore which other conformations might be populated in **2**, the upper distance restraints were implemented in a time-averaged mode in a MD simulation with solvent water present. The use of time-averaged restraints in MD simulations has been proposed[29] and tested,[30,31] as one means to account for the averaging that is inherent in NMR spectroscopic data.

During the MD simulation of **2** with TA-DR the NPNA motif populates predominantly a type-I β-turn. However, it is noteworthy that an Asn^2 NH to Ala^5 CO H-bond is seldom formed. Rather, the most frequently formed H-bond is between the side chain Asn^2 CO(δ) and Ala^5 NH (see Table 5), as seen in Figure 2 and 6. A conformational transition in the template between conformations with the C(γ)−N in a pseudoequatorial position ($\chi_1 \approx -30°$), and a pseudoaxial position ($\chi_1 \approx 0$ to $+30°$), is observed in the simulation (Figures 5 and 6), which is consistent with the averaged ^3J coupling constants observed in the aminoproline moiety of the template in **2** (Table 4). The peptide **8** serves as a useful reference, since here the template is locked into the $\chi_1 \approx +10-20°$ conformation.

Thus the NMR and MD simulation give a self-consistent view of the conformation of the peptide antigen **2**, which includes a stable β-I turn in the NPNA motif but also some flexibility in the template. The β-turn conformation is similar to those found in linear peptides of the type $(NPNA)_3$ and $(NP^{Me}NA)_3$ by NMR and MD methods.[11,12] For example, the backbone N, C(α), and C′ atoms of the residues in the ANPNA loop in a typical structure of **2** (for example, the snapshot at 1.7 ns from the MD simulation) can be superimposed on the central ANP^{Me}NA motif of a typical structure taken from an MD simulation[12] of $(NP^{Me}NA)_3$ with an rmsd of ≈0.6 Å (Figure 9).

For antibody production, the two multiple-antigen-peptides **9** and **10** incorporating the NPNA motif and a single universal T helper cell epitope derived from tetanus toxin[25] were each administered to BALB/c mice together with the adjuvant QS-21. After four booster immunizations, the sera from 12/15 mice immunized with **9** showed specific IgG responses against the immunogen **9**. Some of the elicited IgG from these 12 mice cross-reacted in an immunofluorescence assay (IFA) with *P. falciparum* sporozoites (Figure 8); the remaining mice gave only a response against **9** by ELISA. The binding of anti-**9** serum to sporozoites was inhibited both by the immunogen **9** and by the mimetic **2** (Figure 8). This latter observation is consistent with the specific recognition of sporozoites by anti-**2** antibodies in the sera. In control experiments, cyclic peptides with different sequences mounted on the same template were unable to inhibit antibody binding to sporozoites in the IFA. On the other hand, the sera from none of the mice immunized with **10** (or with adjuvant alone) cross-reacted with sporozoites. Possible reasons for the inactivity of immunogen **10** may include the fact that only a single NPNA motif is present, that its conformational flexibility is high, and/or that its susceptibility to proteolytic degradation in serum is high, in comparison to **9**.

A wider question concerns whether the unnatural template itself is a major epitope in **9**, which could result in the

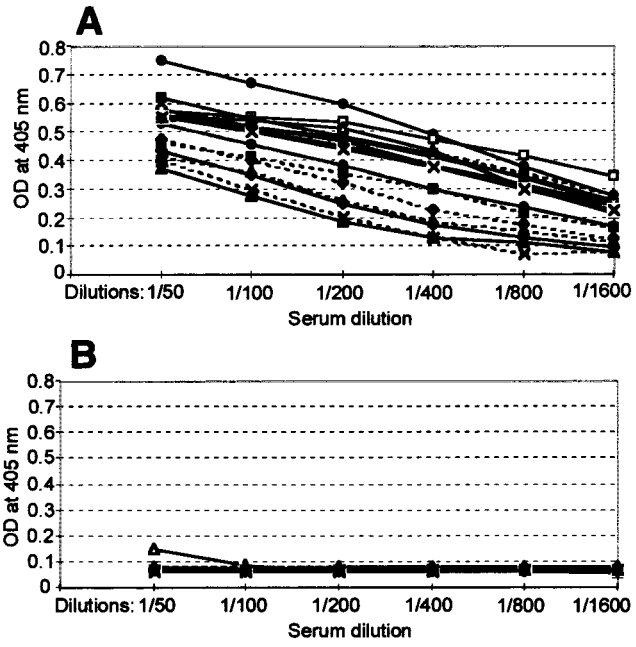

Figure 7. Serum IgG titers of 15 BALB/c mice immunized four times subcutaneously with **9** together with the adjuvant QS-21. ELISA was performed with ELISA microtiter plates coated either with **9** (A) or with **10** (B) and incubated with serial dilutions of the individual mouse sera. Bound IgG was quantitated using alkaline phosphatase conjugated antibodies specific for mouse gamma heavy chains (see Experimental Section).

(29) Torda, A. E.; Scheek, R. M.; van Gunsteren, W. F. *Chem. Phys. Lett.* **1989**, *157*, 289−294.
(30) Pearlman, D. A. *J. Biomol. NMR* **1994**, *4*, 1−16.
(31) Nanzer, A. P.; van Gunsteren, W. F.; Torda, A. E. *J. Biomol. NMR* **1995**, *6*, 313−320.

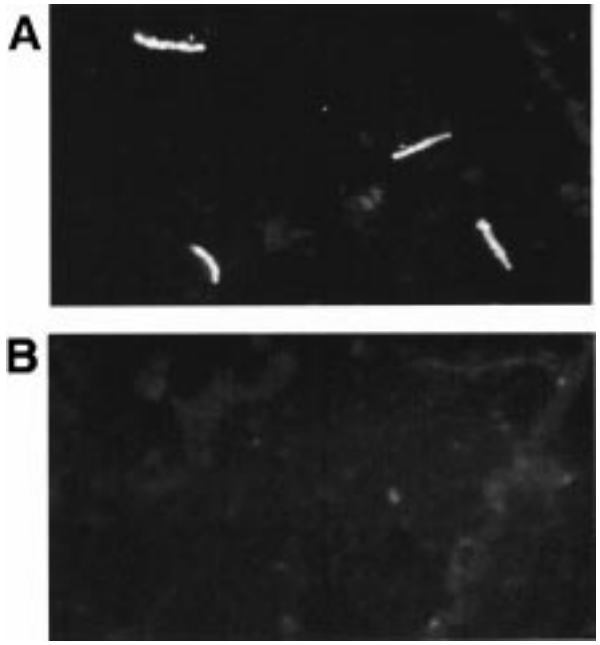

Figure 8. (A) Immunofluorescence staining of *P. falciparum* sporozoites by serum IgG from a mouse immunized with **9** (see Experimental Section for method); (B) Incubation in the presence of the mimetic **2** (50 μg/mL) abolished staining of the sporozoites.

immunological response being directed toward this unnatural antigen. This becomes an issue whenever unnatural templates or amino acids are intended for use in synthetic immunogens but has not been pursued in the present work, where the focus has been on a characterization of the antigen conformation and the anti-NPNA response elicited by **9**.

The finding that a single NPNA motif in the form of a cyclic peptide, constrained into a β-I turn conformation, can elicit anti-sporozoite antibodies provides additional support for the immunological relevance of the NPNA cadence in the repeat region of the CS protein and provides a direct correlation between a β-I turn conformation in the free antigen and immune recognition of the parasite. However, the free antigen **2** is not rigid (vide supra) and as yet the antibody-bound conformation(s) is(are) not known. By introducing the conformational constraint, the specificity of the immune response to the NPNA repeat is undoubtedly more stringent than would be the case with a linear peptide immunogen. For this reason, the ability of **9** to elicit anti-sporozoite antibodies is significant. With the multiple-antigen-peptide construct used here, the immunogenicity of **2** was low, and anti-**2** serum IgG titers increased only gradually with each booster immunization. However, this will be influenced also by the type and copy number of the T-helper cell epitope in the immunogen. Improved immunogenicity can be expected by conjugation to a carrier containing multiple T-cell epitopes. It was noted earlier,[27,32] that the fine specificity of antibodies to the repeat sequence of the CS protein could be manipulated by using sequence variants of $(NANP)_n$. In particular, the major epitopes in the repeat region on the parasite seem from serological studies[32−34] to encompass at least two or three NANP repeats. This implies the adoption of more complex, immunologically relevant structures in longer tandem repeat peptides. Earlier MD studies[12] of $(NP^{Me}NA)_3$ peptides indicated how longer tandem repeat peptides might begin to fold and hence what structures the major epitope(s) might adopt. In particular, the NPNA motif was seen to define not only a sequence repeat but also a conformational repeat, which could be used for the assembly of larger epitopes on the native CS protein. The results reported here certainly strengthen the conclusion that a β-I turn is the major conformational epitope within the NPNA motif.

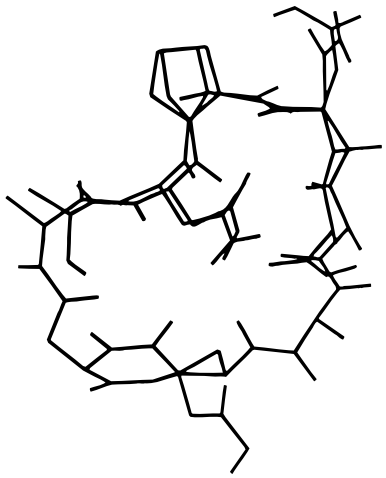

Figure 9. Superimposition (over the N, C(α), and C′ atoms) of the ANPNA sequence in a snapshot from the MD simulation of **2** (at 1.7 ns), with the central $ANP^{Me}NA$ motif taken from an earlier MD simulation[12] of the linear peptide $(NP^{Me}NA)_3$.

Experimental Section

Methyl (2*S*,4*R*)-4-Hydroxyprolinate Hydrochloride. To a suspension of (2*S*,4*R*)-4-hydroxyproline (60.0 g, 458 mmol) in MeOH (550 mL) was added thionyl chloride (68 mL, 937 mmol) at 0 °C. The resulting suspension was stirred 30 min at room temperature and then refluxed for 4 h. Evaporation of solvent gave product (82.8 g, 99%) which was used without further purification. For analytical purposes the product was recrystallized from Et_2O/MeOH (93%). Mp 162−164°. $[\alpha]_D^{21} = -24.3$ (*c* 1.05, MeOH). ^{1}H NMR (300 MHz, (D_6)DMSO): 2.09 (*ddd*, *J* = 13.3, 10.9, 4.5, 1 H); 2.20 (*dddd*, *J* = 13.3, 7.5, 1.6, 1.6, 1 H); 9.96 (br., 2 H); 3.07 (*ddd*, *J* = 12.3, 1.6, 1.6, 1 H); 3.37 (*dd*, *J* = 12.1, 4.5, 1 H); 3.76 (*s*, 3 H); 4.42−4.40 (*m*, 1 H); 4.45 (*dd*, *J* = 10.9, 7.4, 1 H); 5.64 (br., 1H). CI-MS (NH_3): 146.2 (100, [M + H]).

(2*S*,4*R*)-*N*-[(Benzyl)oxycarbonyl]-4-hydroxy-L-proline Methyl Ester. To the foregoing product (41.0 g, 225.7 mmol) in dioxane (250 mL) and 1 M aqueous Na_2CO_3 (500 mL) at 0 °C was added benzyloxycarbonyl chloride (50.3 mL, 339 mmol). The mixture was stirred 1 h at 0 °C and overnight at room temperature. After acidifying to pH 2, extraction with EtOAc, washing with brine and water, and drying ($MgSO_4$), the solvent was evaporated. The residue was purified by column chromatography (silica, EtOAc/hexane 1:1, then EtOAc/hexane 2:1) to yield product (51.7 g, 84%) as a colorless oil. $[\alpha]_D^{21} = -57.1$ (*c* 1.0, CH_2Cl_2). ^{1}H NMR (300 MHz, $CDCl_3$): 2.05 (*m*, 1H); 2.28 (*m*, 1H); 2.69 (*s*, 1H); 3.63 (*m*, 2H); 3.53 (*s*, 9/5H), 3.73 (*s*, 6/5H); 4.48 (*m*, 2H); 4.98 (*d*, *J* = 12.5, 3/5H); 5.09 (*d*, *J* = 12.5, 2/5H); 5.14 (*d*, *J* = 12.5, 2/5H); 5.16 (*d*, *J* = 12.5, 3/5H). CI-MS (NH_3): 297 (11, $[M + NH_4]^+$), 280 (100, $[M + H]^+$).

(2*S*,4*R*)-*N*-[(Benzyl)oxycarbonyl]-4-[(trimethylsilyl)oxy]-L-proline Methyl Ester. To the foregoing product (47.4 g, 170 mmol) in THF (420 mL) were added NEt_3 (118.4 mL, 849.0 mmol) and trimethylsilyl chloride (53.7 mL, 424.5 mmol). A white precipitate was formed. After 21 h the suspension was filtered and the filtrate was washed with Et_2O. The etheral solution was washed with 1 M aqueous Na_2CO_3 (500 mL), dried ($MgSO_4$), and evaporated to afford the silyl ether as a clear orange oil (59.7 g, 100%). ^{1}H NMR (300 MHz, $CDCl_3$): 0.13 (*s*, 9H); 2.20−2.10 (*m*, 1H); 2.16−2.26 (*m*, 1H);

(32) DelGiudice, G.; Tougne, C.; Renia, L.; Ponnudurai, T.; Corradin, G.; Pessi, A.; Verdini, A. S.; Louis, J. A.; Mazier, D.; Lambert, P.-H. *Mol. Immunol.* **1991**, *9*, 1003−1009.

(33) Zavala, F.; Tam, J. P.; Hollingdale, M. R.; Cochrane, A. H.; Quakyi, I.; Nussenzweig, R. S.; Nussenzweig, V. *Science* **1985**, *228*, 1436−1440.

(34) Togna, A. R.; DelGiudice, G.; Verdini, A. S.; Bonelli, F.; Pessi, A.; Engers, H. D.; Corradin, G. *J. Immunol.* **1986**, *137*, 2956−2960.

3.42 (*dd*, $J = 11.0$, $J = 3.0$, 0.5H); 3.50 (*dd*, $J = 11.0$, $J = 1.6$, 0.5H); 3.70 (*dd*, $J = 11.0$, $J = 5.0$, 1H); 3.67, 3.77 (2*s*, 3H); 4.31−4.52 (*m*, 2H); 5.04 (*d*, $J = 12.5$, 0.5H); 5.12 (*d*, $J = 12.5$, 0.5H); 5.20 (*d*, $J = 12.5$, 0.5H); 5.22 (*d*, $J = 12.5$, 0.5H); 7.21−7.40 (*m*, 5H).

(2*S*,4*R*) and (2*S*,4*S*)-*N*-[(Benzyl)oxycarbonyl]-2-{[(*tert*-butyl)oxycarbonyl]methyl}-4-hydroxyproline Methyl Ester (3) and (3′). To a solution of diisopropylamine (35.5 mL, 250.2 mmol) in anhydrous THF (370 mL) at −5 °C was added *n*-BuLi (133.7 mL, 213.9 mmol, 1.6 M in hexane). After stirring for 15 min at −5 °C the solution was cooled to −70 °C. A solution of the foregoing silyl ether (62.9 g, 178.7 mmol) in anhydrous THF (150 mL) was added dropwise and stirred for 30 min at −70 °C, and then *tert*-butyl-2-bromoacetate (45.5 mL, 304 mmol) was added dropwise. After 15 min at −70 °C, 90 min at 0 °C, and overnight at room temperature, the reaction mixture was poured into saturated aqueous NH_4Cl (400 mL) and extracted with EtOAc (3 × 500 mL). The combined organic fraction was dried ($MgSO_4$) and evaporated to yield a dark brown oil (97.7 g). This was dissolved in a methanolic citric acid solution (500 mL, 10%) and stirred 3 h at room temperature. Then 250 mL of EtOAc was added, and the MeOH was partly evaporated. After addition of EtOAc and washing with 1 M aqueous Na_2CO_3, the organic fraction was dried ($MgSO_4$) and evaporated, and the residue was chromatographed (silica, EtOAc/hexane 1:2) to yield a diastereomeric mixture of **3** and **3′** as a brown oil (52.6 g, 72%). CI-MS (NH_3): 411 (25, $[M + NH_4]^+$), 294 (100, $[M + H]^+$).

(2*S*,4*R*) and (2*S*,4*S*)-*N*-[(Benzyl)oxycarbonyl]-2-{[(*tert*-butyl)oxycarbonyl]methyl}-4-phthalimidoproline Methyl Ester. To the foregoing product (13.0 g, 33.0 mmol), phthalimide (14.6 g, 99.0 mmol), and PPh_3 (21.6 g, 82.5 mmol) in THF (400 mL) at −25 °C was added diethyl azodicarboxylate (11.3 mL, 72.6 mmol). After 3 h at −25°, and at room temperature overnight, the solvent was removed in vacuo, and the residue was purified by column chromatography (silica, EtOAc/hexane, 1:2). The remaining phthalimide was precipitated from AcOEt/hexane 1:3, and evaporation of the mother liquor yielded the two diastereoisomers as a viscous brown oil (12.1 g, 70%). CI-MS (NH_3): 523 (100, $[M + H]^+$).

(2*S*,4*R*) and (2*S*,4*S*)-2-{[(*tert*-Butyl)oxycarbonyl]methyl}-4-phthalimidoproline Methyl Ester (4 and 4′). The foregoing phthalimides (11.31 g, 13.4 mmol) in DMF (180 mL) with Pd/C (2.32 g, 10% Pd) were stirred 4 days at room temperature and 1 atm under H_2. The solvent was removed in vacuo, the residue was dissolved in CH_2Cl_2, and filtered through a Celite pad, and the solvent evaporated to give **4** and **4′** as a slightly yellow solid. This residue was dissolved in the minimum volume of CH_2Cl_2 (61 mL) and 1.5 times this volume hexane (92 mL) was added. This mixture was seeded with pure diastereoisomer **4** and left at 4 °C overnight. The resulting white precipitate was collected and washed to give **4** (3.46 g, 41.2%). The mother liquor was evaporated, and crystallization of the residue from hot hexane gave diastereoisomer **4′** as a white solid. Repeating this procedure on mother liquors gave additional **4** (yield 47%) and **4′** (yield 23%). **4**: Mp 181−183°. $[\alpha]_D^{21} = -14.0$ (*c* 1.03, CH_2Cl_2). IR (KBr): 3460w (br.), 3355m, 3010w, 2970m, 2900w, 1770m, 1730s, 1710s, 1615w. ^{1}H NMR (300 MHz, $CDCl_3$): 1.37 (*s*, 9H); 2.17 (*dd*, $J = 13.7$, $J = 10.0$, 1H); 2.58 (*d*, $J = 15.7$, 1H); 2.63 (*dd*, $J = 13.7$, $J = 7.5$, 1H); 2.93 (*d*, $J = 15.7$, 1H); 3.22 (*dd*, $J = 9.4$, $J = 8.0$, 1H); 3.51 (*dd*, $J = 9.4$, $J = 9.0$, 1H); 3.80 (*s*, 3H); 4.85 (*ddd*, $J = 10.0$, 9.0, 8.0, 1H); 7.64 and 7.74 (2*m*, 2 × 2H). ^{13}C NMR (75.4 MHz, $CDCl_3$): 27.9; 38.1; 45.6; 48.4; 48.8; 52.6; 66.1; 81.2; 123.2; 131.7; 134.0; 167.8; 169.5; 175.1. CI-MS (NH_3): 389 (100, $[M + H]^+$). Anal. Calc. for $C_{20}H_{24}N_2O_6$ (388.42): C 61.9, H 6.2, N 7.2. Found: C 62.0, H 6.2, N 7.3. **4′**: Mp 110−111°. $[\alpha]_D^{21} = -20.4$ (*c* 1.02, CH_2Cl_2). IR (KBr): 3450w (br.), 3335w, 2965w, 1775w, 1735s, 1710s, 1695s. ^{1}H NMR (300 MHz, $CDCl_3$): 1.43 (*s*, 9H); 2.42 (*dd*, $J = 13.2$, $J = 9.1$, 1H); 2.54 (*dd*, $J = 13.2$, $J = 8.9$, 1H); 3.00 (*s*, 2H); 3.37 (*dd*, $J = 11.0$, $J = 7.5$, 1H); 3.43 (*dd*, $J = 11.0$, $J = 8.5$, 1H); 4.82 (*ddd*, $J = 8.8$, 8.5, 7.2, 1H); 7.72 and 7.83 (2*m*, 2 × 2H). ^{13}C NMR (75.4 MHz, $CDCl_3$): 27.9; 38.5; 44.3; 48.8; 49.5; 52.6; 67.1; 81.2; 123.2; 131.7; 134.0; 168.0; 169.8; 174.9. CI-MS (NH_3): 389 (100, $[M + H]^+$).

Allyl ((2*S*,6*S*,8a*S*)-8a{[(*tert*-Butyl)oxycarbonyl]methyl}perhydro-5,8-dioxo-2-phthalimidopyrrolo[1,2-*a*]pyrazine-6-acetate (5). To a suspension of **4** (2.00 g, 5.15 mmol), HOAt (1.40 g, 10.3 mmol), and DCC (2.14 g, 10.3 mmol) in CH_2Cl_2 (40 mL) at room temperature was added Fmoc-L-Asp(OAllyl)-OH (4.07 g, 10.3 mmol) in CH_2Cl_2 (28 mL). After stirring 24 h, the solution was filtered and evaporated. The resulting yellow foam was dissolved in a solution of DBU in MeCN (5% v/v, 24 mL), stirred for 8 h, then diluted with CH_2Cl_2 (70 mL), and washed first with 10% aqueous citric acid and then brine, and the combined organic fractions were dried ($MgSO_4$) and evaporated. The residue was redissolved in CH_2Cl_2, filtered to remove dicyclohexyl urea, evaporated, and then purified by flash chromatography (EtOAc/hexane 1:1) to afford **5** as a white solid (1.69 g, 64%). Mp 191−192°. $[\alpha]_D^{21} = -32.3$ (*c* 0.99, $CHCl_3$). IR (KBr): 3450w (br.), 3360m, 2980m, 2930w, 1770m, 1725s, 1710s, 1675s, 1660s, 1615w, 1440m, 1380s. ^{1}H NMR (300 MHz, $CDCl_3$): 1.45 (*s*, 9H); 2.58 (*dd*, $J = 13.7$, $J = 9.0$, 1H); 2.69 (*d*, $J = 16.0$, 1H); 2.77 (*dd*, $J = 13.7$, $J = 7.0$, 1H); 2.91 (*dd*, $J = 17.7$, $J = 10.8$, 1H); 3.03 (*d*, $J = 16.0$, 1H); 3.47 (*dd*, $J = 17.7$, $J = 3.1$, 1H); 3.72 (*dd*, $J = 13.2$, $J = 9.0$, 1H); 4.34 (*dd*, $J = 13.2$, $J = 3.7$, 1H); 4.68 (*d*, $J = 5.8$, 1H); 4.73 (*dd*, $J = 10.8$, 3.1, 1H); 5.08 (*dddd*, $J = 9.1$, 8.9, 7.0, 3.7, 1H); 5.37 (*d*, $J = 17.2$, 1H); 5.95 (*ddt*, $J = 17.2$, 10.3, 5.8, 1H); 6.76 (*s*, 1H); 7.70 and 7.82 (2*m*, 2 × 2H). ^{13}C NMR (75.4 MHz, $CDCl_3$): 27.9; 36.8; 40.4; 42.2; 45.4; 48.9; 52.3; 65.8; 82.1; 118.8; 123.5; 131.5; 134.2; 164.0; 167 0.4; 168.3; 169.2; 171.4. ES-MS (NaI): 534.5 (100, $[M + Na]^+$). Anal. Calc. for $C_{26}H_{29}N_3O_8$ (511.54): C 61.0, H 5.7, N 8.2. Found: C 60.6, H 5.7, N 8.2.

Allyl ((2*S*,6*S*,8a*S*)-8a-[(*tert*-butyl)oxy)carbonyl]methyl}perhydro-5,8-dioxo-2-[(fluorenyl)methyloxycarbonyl]pyrrolo[1,2-*a*]pyrazine-6-acetate (1). To a solution of **5** (2.00 g, 3.91 mmol) in DMF (20 mL) was added methylhydrazine (800 μL, 15.2 mmol). After stirring 4.5 h at 60 °C, the solvent was removed in vacuo, the residue was redissolved in CH_2Cl_2 and filtered, and the solvent evaporated. The residue in CH_2Cl_2 (20 mL) was treated with Fmoc-succinimide (2.64 g, 7.83 mmol), imidazole (0.47 g, 7.83 mmol), and DMAP (48 mg, 3.93 mmol) and stirred for 3 h at room temperature. After washing with aqueous citric acid (0.1%) and brine and drying ($MgSO_4$), the solvent was evaporated, and the residue was purified by chromatography (silica, EtOAc/hexane 3:2) to give the corresponding amine (1.37 g, 58%) as a white powder. IR (film): 3386w, 3008m, 3015w, 1728s, 1682s, 1518m, 1450s, 1155 s. ^{1}H NMR (300 MHz, $CDCl_3$): 1.45 (*s*, 9H); 2.58 (*dd*, $J = 13.7$, $J = 9.0$, 1H); 2.69 (*d*, $J = 16.0$, 1H); 2.77 (*dd*, $J = 13.7$, $J = 7.0$, 1H); 2.91 (*dd*, $J = 17.7$, $J = 10.8$, 1H); 3.03 (*d*, $J = 16.0$, 1H); 3.47 (*dd*, $J = 17.7$, $J = 3.1$, 1H); 3.72 (*dd*, $J = 13.2$, $J = 9.0$, 1H); 4.34 (*dd*, $J = 13.2$, $J = 3.7$, 1H); 4.68 (*d*, $J = 5.8$, 1H); 4.73 (*dd*, $J = 10.8$, 3.1, 1H); 5.08 (*dddd*, $J = 9.1$, 8.9, 7.0, 3.7, 1H); 5.37 (*d*, $J = 17.2$, 1H); 5.95 (*ddt*, $J = 17.2$, 10.3, 5.8, 1H). ^{13}C NMR (75 MHz, $CDCl_3$): 27.89; 36.24; 42.32; 43.32; 47.08; 47.83; 51.41; 52.07; 65.16; 65.76; 66.77; 82.01; 118.83; 119.89; 124.91; 126.99; 127.64; 131.42; 141.19; 143.71; 155.83; 164.91; 168.42; 169.96; 170.44. ES-MS (NaI): 626.4 (100, $[M + Na]^+$). The foregoing amine (1.00 g, 1.66 mmol) in CH_2Cl_2 (2 mL) and TFA (4 mL) was stirred at room temperature and then evaporated, and dioxane was added and evaporated to remove traces of TFA. The residue was purified by chromatography (silica, EtOAc, then EtOH) to yield product (880 mg, 97%) as a white hygroscopic powder. IR (film): 3378s (br.), 3007m, 2966m, 2859m, 1719s, 1745s, 1452s, 1177s, 1121 s. ^{1}H NMR (300 MHz, $CDCl_3$): 1.44 (*s*, 9H); 2.25 (*dd*, $J = 14.0$, 6.0, 1H); 2.59 (*dd*, $J = 14.0$, 7.5, 1H); 2.59 (*dd* $J = 16.0$, 7.3, 1H); 2.98 (*d*, $J = 16.0$, 1H); 3.04 (*m*, 2H); 3.62 (*dd*, $J = 13.0$, 7.0, 1H); 4.05 (br. *d*, $J = 13.0$, 1H); 4.20 (*t*, $J = 7.0$, 1H); 4.39 (*d*, $J = 7.0$, 2H); 4.35−4.50 (*m*, 2H); 4.52 (*m*, 2H); 5.26 (*d*, $J = 10.5$, 1H); 5.30 (*d*, $J = 17.5$, 1H); 5.94 (*d*, $J = 8.5$, 1H); 5.89 (*dddd*, $J = 17.5$, 10.5, 5.5, 4.5, 1H); 6.27 (*s*, 1H); 7.31 (*m*, 2H); 7.40 (*m*, 2H); 7.58 (*d*, $J = 7.3$, 2H); 7.76 (*d*, $J = 7.5$). ^{13}C NMR (75 MHz, $CDCl_3$): 35.95; 40.50; 42.56; 46.89; 47.57; 51.04; 52.13; 60.89; 64.87; 65.87; 66.91; 118.77; 119.88; 124.86; 126.99; 127.67; 131.23; 141.13; 143.55; 156.33; 160.88; 165.48; 170.70; 172.64. ES-MS (NaI): 570.5 (100, $[M + Na]^+$).

Peptide Synthesis. Loop 2. Tentagel-S AC resin (Rapp Polymere, Tübingen) (1.0 g, 0.23 mmol/g) in CH_2Cl_2 and pyridine (3 mL, 1:1) was treated with **1** (0.38 g, 3 equiv) and 2-chloro-1,3-dimethylimidazolidinium hexafluorophosphate (CIP) (386 mg, 6 equiv) with swirling for 1.5 h. The resin was then filtered and washed successively with CH_2Cl_2, methanol, and CH_2Cl_2. The substitution level of template on

the resin was 65% (0.15 mmol/g). The Fmoc group was removed with piperidine in DMF (20%), and the amino acids Fmoc-Ala-OH, Fmoc-Ala-OH, Fmoc-Asn(Mtt)-OH, Fmoc-Pro-OH, Fmoc-Asn(Mtt)-OH, and Fmoc-Ala-OH were added sequentially using standard solid-phase methods.[17] The allyl ester was removed by treating resin-bound peptide with $Pd(PPh_3)_4$ (345 mg, 2 equiv), *N*-methylmorpholine (0.3 mL), and AcOH (0.6 mL) in DMF (12 mL) under oxygen-free conditions. After 2 h, the resin was filtered and washed successively with CH_2Cl_2, diisopropylethylamine in DMF (0.5% v/v), sodium diethyldithiocarbamate in DMF (0.5%), methanol, and finally CH_2Cl_2. Deprotection was monitored by reverse-phase HPLC (C_{18} column, eluting with a gradient from 0 to 100% MeCN in H_2O + 0.1% TFA). The N-terminal Fmoc group was then removed with piperidine in DMF (20%), and cyclization was performed with benzotriazol-1-yloxy-tris(dimethylamino)phosphonium hexafluorophosphate (BOP) (61 mg, 1.5 equiv) in *N*-methylpyrrolidone-DMSO (9 mL, 4:1) and diisopropylethylamine (65 μL, 3 equiv) for 1.5 h. Upon completion, the peptide was cleaved from the resin with TFA-triisopropylsilane−H_2O (95:2.5:2.5) and purified by reverse-phase HPLC (see above for conditions) to give **2** (20.0 mg) (EI-MS: 806.5 (100, $[M + H]^+$)) and a dimer (EI-MS: 1612 (100, $[M + H]^+$)).

Loop 8. This loop was made following the same procedure as used for **2**, except for the use of Fmoc-Cys(Trt)-OH in peptide assembly. After cleaving the cyclic peptide from the resin with TFA−thioanisole−1,2-ethanedithiol−H_2O−triisopropylsilane (87.5:5:2.5:2.5:2.5), air oxidation of the free dithiol in ammonium acetate buffer (pH 8), monitored by reverse phase HPLC, gave **8** (5.6 mg, 8%) (EI-MS: 868.4 (36, $[M + H]^+$)).

Multiple-Antigen-Peptides. The peptide H_4-$(Lys)_2$-Lys-Ala-Ala-Gln(Mtt)-Tyr(*t*Bu)-Ile-Lys(Boc)-Ala-Asn(Mtt)-Ser(*t*Bu)-Lys(Boc)-Phe-Ile-Gly-Ile-Thr(*t*Bu)-Glu(O*t*Bu)-Leu-Ala was assembled on Tentagel-S AC resin using standard methods.[17] The loop **2** (60 mg, 3 equiv) was then coupled to this resin (47 mg, with 0.025 mmol free amino groups) using *O*-(benzotriazol-1-yl)-*N*,*N*,*N*′,*N*′-tetramethyluronium hexafluorophosphate (HBTU) (28 mg, 3 equiv) and 1-hydroxybenzotriazole (HOBt) (9.4 mg, 3 equiv) in *N*-methylpyrrolidone (0.6 mL) and diisopropylethylamine (19.4 μL) overnight at room temperature. The product **9** was cleaved from the resin with TFA−triisopropylsilane−H_2O (95:2.5:2.5) and purified by reverse-phase HPLC (see above for conditions) (5.2 mg). EI-MS: 5475.0 (100, $[M + H]^+$). The peptide **10** was assembled by standard solid-phase methods,[17] and purified in the same way.

NMR and Structure Calculations. For the peptides **2** and **8**, ^{1}H 2D ROESY, TOCSY, and DQF−COSY spectra were recorded in H_2O/D_2O (90:10), pH 5, at 600 MHz (Bruker AMX600 spectrometer), typically at a concentration of ≈20 mg/mL. The water signal was presaturated, and 2D spectra were acquired with 2048 × 512 points, except for determination of coupling constants from an E.COSY spectrum measured with 8192 × 512 points. NMR spectra were processed and analyzed using Felix software (MSI, San Diego).

To derive NOE distance restraints it was assumed that the initial rate approximation is valid and that each peptide rotates as a single isotropic rotor. The NOE connectivities for **2** were determined from a series of ROESY spectra with mixing times of 40, 80, 120, and 200 ms and for **8** using 50, 100, 150, and 250 ms mixing times. Cross-peak volumes were determined by integration, and the build-up curves were checked to ensure a smooth exponential increase in peak intensity for all NOEs used in deriving distance restraints, as a selection criterion for cross-peak intensities due to direct NOEs and not the product of, for example, TOCSY-type coherence pathways combined with cross-relaxation.

The relative cross-peak volumes were assumed to be proportional to r^{-6} and were used to derive distance restraints for simulated annealing (SA) calculations and MD simulations. In the case of peptide **2**, the ROESY series was measured at 300 and at 285 K. The same distance restraints were determined (within a margin of ≈10%) at both temperatures, so the minor conformer of **2** should make a negligible contribution to the NOEs measured for the major conformer (see Results section−exchange rates). The minor conformer was not investigated further. SA calculations were performed to derive average solution structures, using methods described in detail elsewhere.[21]

For the MD simulation of **2** with and without TA-DR the GROMOS96 suite of programs was used, with the 43A1 force field for simulations with solvent water.[23] The 27 upper distance restraints used were the exact values obtained from ROE build-up curves, with a memory decay time $\tau_{dr} = 100$ ps and a force constant $K_{dr} = 1000$ kJ mol^{-1} nm^{-2}. The starting structure was the lowest energy SA structure in a truncated octahedral box (box length 41.42 Å) with 1142 SPC water molecules. The temperature was held constant by weak coupling ($\tau_T = 0.1$ ps) to an external bath at 300 K. The SHAKE algorithm was used to maintain bond lengths with a relative precision of 10^{-4} and the integrator time step was 0.002 ps. Nonbonded interactions evaluated at every step were within a short-range cutoff of 8 Å. For long-range interactions the cutoff was 14 Å. Structures were saved for analysis every 100 steps (0.2 ps). After short simulations to relax the solute and solvent, the simulations with and without TA-DR were each run for 2 ns.

Immunization of Mice. Two groups of 15 female BALB/c mice, six to eight weeks old, were immunized subcutaneously with 50 μg of **9** or **10** in phosphate-buffered saline (100 μL) (pH 6.7) containing 20 μg of the adjuvant QS-21.[35] As a control, a third group of five mice received 20 μg of QS-21 in PBS (100 μL). Mice were immunized four times at two week intervals and a fifth time 2 months after the fourth immunization. Mice were bled by retroorbital puncture before the first immunization and 11−14 days after the third, fourth, and fifth immunizations. Blood was collected and incubated at 37 °C for 1 h and at 4 °C for 3 h, and the cells were then removed by centrifugation.

Enzyme-Linked Immunosorbent Assay (ELISA). ELISA microtiter plates (Immunolon 4B, Dynatech, Switzerland) were coated at 4 °C overnight with a solution of **9** or **10** in PBS (50 μL of 5 μg/mL, pH 7.2). Wells were then blocked with 5% milk powder in PBS for 1 h at 37 °C and washed three times with PBS containing 0.05% Tween-20 (Merck, Germany). Plates were then incubated with serial dilutions of mouse serum in PBS containing 0.05% Tween-20 and 0.5% milk powder (dilution buffer) for 2 h at 37 °C. After washing, the wells were incubated with alkaline phosphatase conjugated-goat anti-mouse IgG (γ-chain specific) antibodies (62 ng/mL in dilution buffer) for 2 h at 37 °C and then washed. Phosphatase substrate (*p*-nitrophenyl phosphate) (1 mg/mL) in buffer (Na_2CO_3 (1.4 g/L) $NaHCO_3$ (3 g/L) and $MgCl_2 \cdot 6H_2O$ (0.2 g/L), pH 9.6) was added and incubated at room temperature. After 1 h the absorbance was measured at 405 nm (Figure 7).

Immunofluorescence Assays. IFA were performed as described elsewhere.[36] Briefly, air-dried unfixed *P. falciparum* salivary gland sporozoites (strain NF54) attached to microscope glass slides were incubated in a moist chamber for 20 min at 37 °C with serum diluted in PBS. The slides were then washed five times with PBS containing 0.1% bovine serum albumin (PBS−BSA) and dried. FITC-labeled goat anti-mouse IgG (Fab-specific) antibodies (Sigma), diluted to 46 μg/mL in PBS (pH 7.2) containing 0.1 g/L Evans-Blue (Merck, Germany), were added. After incubation for 20 min at 37 °C the slides were again washed five times with PBS−BSA, dried, and covered with glycerol and a cover-slide. A Leitz Dialux 20 microscope using 12.5/18 ocular and a 40x/1.30 oil fluorescence 160/0.17 objective was used to detect fluorescence staining at 495 nm excitation and 525 nm emission wavelengths. For competition experiments, serum was diluted 1:10 and incubated with cyclic peptides at final concentrations of 500 μg/mL or 50 μg/mL for 1 h at 37 °C prior to staining. Both concentrations yielded comparable results for each peptide tested.

Acknowledgment. This work was supported by grants from the Swiss National Science Foundation and the Roche Research Foundation. We thank Prof. van Gunsteren for providing the GROMOS96 suit of programs for computer simulations.

JA980444J

(35) Kensil, C. R.; Soltysik, S.; Wheeler, D. A.; Wu, J. Y. *Adv. Exp. Med. Biol.* **1996**, *404*, 165−172.

(36) Boulanger, N.; Matile, H.; Betschart, B. *Acta Trop.* **1988**, *45*, 55−65.

(37) Kraulis, P. J. *J. Appl. Cryst.* **1991**, *24*, 946−950.